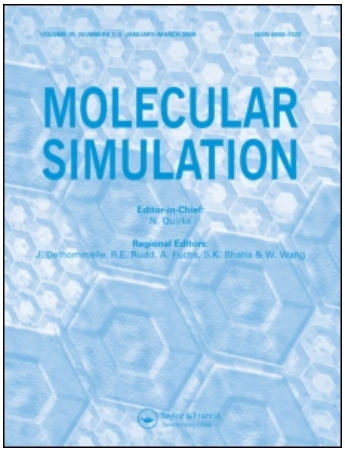


**Molecular Simulation**
Publication details, including instructions for authors and subscription information:
http://www.informaworld.com/smpp/title~content=t713644482

# Molecular dynamic study of subtilisin Carlsberg in aqueous and nonaqueous solvents

Anthony Cruz[a]; Eunice Ramirez[a]; Alberto Santana[a]; Gabriel Barletta[b]; Gustavo E. López[a]
[a] Chemistry Department, University of Puerto Rico, Mayaguez, Puerto Rico [b] Department of Chemistry, University of Puerto Rico at Humacao, Humacao, Puerto Rico

**To cite this Article** Cruz, Anthony , Ramirez, Eunice , Santana, Alberto , Barletta, Gabriel and López, Gustavo E.(2009) 'Molecular dynamic study of subtilisin Carlsberg in aqueous and nonaqueous solvents', Molecular Simulation, 35: 3, 205 — 212
**To link to this Article: DOI:** 10.1080/08927020802415670
**URL:** http://dx.doi.org/10.1080/08927020802415670

*Molecular Simulation*
Vol. 35, No. 3, March 2009, 205–212

Taylor & Francis
Taylor & Francis Group

# Molecular dynamic study of subtilisin Carlsberg in aqueous and nonaqueous solvents

Anthony Cruz[a1], Eunice Ramirez[a]*, Alberto Santana[a2], Gabriel Barletta[b3] and Gustavo E. López[a4]

[a]*Chemistry Department, University of Puerto Rico, Mayaguez, Puerto Rico;* [b]*Department of Chemistry, University of Puerto Rico at Humacao, Humacao, Puerto Rico*

(*Received 28 March 2008; final version received 17 August 2008*)

Using molecular dynamics simulations, we have obtained an important insight into the structural and dynamical changes exerted by a nonaqueous solvent on the serine protease subtilisin Carlsberg. Our findings show that the structural properties of the subtilisin–acetonitrile (MeCN) system were sensitive to the amount of water present at the protein surface. A decrease or lack of water promoted the enzyme–MeCN interaction, which increased structural changes of the enzyme primarily at the surface loops. This effect caused variations on the secondary and tertiary structure of the protein and induced the opening of a pathway for the solvent to the protein core. Also, disturbance of the oxyanion hole was observed due to changes in the orientation in the Asn-155 side chain. The disruption of the oxyanion hole and the changes of the tertiary structure should affect the optimal activity of the enzyme.

**Keywords:** enzyme catalysis; essential waters; enzyme stability



## 1. Introduction

Research endeavours associated with non-aqueous enzymology have found their way into all areas of chemistry, including biomedical research, as enzymes have been successfully used for the synthesis of bio-relevant compounds [1]. The study of enzymes in non-aqueous media is a particularly exciting field of research due to all the advantages that such media introduce. These include the increased solubility of hydrophobic substrates, favourable shifts of reaction equilibrium [2], increased thermostability of enzymes [3], minimisation of side reactions [4], altered substrate specificity and the ability to perform reactions that are kinetically or thermodynamically unfavourable in water [5].

There are still major drawbacks that preclude us from using enzymes to their full potential. Particular issues are the fact that enzymes are frequently less active in organic solvents than in water [6], that they lose most of their activity after prolonged exposure to organic solvents [1] and that there is a lack of predictability of enantio- and regioselectivity of the enzymes [7]. The decrease in enzymatic activity could be driven by the nature of the solubilisation processes used to maintain the enzyme in an organic environment. Also, various factors including water content, solvent polarity, enzyme flexibility, metals and salt interactions, changes in structure and reaction pathways [8] could be related to the changes in the enzyme activity. As a consequence of all the factors mentioned above, the trial-and-error method remains the most effective approach to achieve the desired reaction outcome.

It is known that the hydration per cent of the media greatly influences the dynamics and activity exhibited by an enzyme. Micaelo and collaborators applied molecular dynamics/molecular mechanics methodologies to study the enzyme cutinase in hexane with various hydration conditions (0–25% w/w). They found that at low amounts of water (0–2.5% w/w) the enzyme is extremely rigid, whereas at higher water content (over 25% w/w) the protein will be denaturalised because of an increase in its flexibility. On the other hand, with a 5–10% w/w of water the structural and dynamic properties of cutinase resemble the native form, with a higher enzymatic activity [9]. In addition, they showed that water exerts control on the enantioselectivity of this enzyme, which preferentially stabilises the R enantiomer in the range of 5–10% w/w of water [10]. Recently, a similar behaviour was observed with the serine protease cutinase in an ionic liquid environment [11]. As observed with hexane, the optimum hydration condition for the protein was 5–10%, with higher hydration percentages denaturising the enzyme. Furthermore, the protein displays a bell-shape-like behaviour relative to the amount of water present, the same that occurs in organic solvents. This result suggested that the processes observed in the enzyme are very similar in the organic and ionic liquid medium. However, the stability of the enzyme in an ionic liquid medium depends directly on the nature of the anionic species selected.

*Corresponding author. Email: eramirez@uprm.edu

ISSN 0892-7022 print/ISSN 1029-0435 online

DOI: 10.1080/08927020802415670
http://www.informaworld.com

Another important factor related to the stability of enzymes is the polarity of the media. Micaelo and Soares [12] found that as the polarity of the solvent increases the amount of water necessary to observe native-like structure also increases. They also established that the polarity of the solvent affects the behaviour of the water at the protein surface. A dramatic decrease of subtilisin BPN' [13] and subtilisin C [6] activity has been observed experimentally as the polarity of the organic solvent increases. To understand this behaviour at a molecular level, molecular dynamics simulations have been performed to mimic the experimental conditions of subtilisin BPN'. In the simulations, the enzyme was exposed to three different solvent environments (octane, tetrahydrofurane and acetonitrile (MeCN)) of increasing polarity. In the timescale of the simulations it was found that the solvent did not affect the overall structure and flexibility of the enzyme when compared to the enzyme in the aqueous media. The most appreciable difference between the systems was the partitioning of the 'essential water molecules' between the enzyme surface and the bulk solvent. It was observed that segregation of the water molecules to the surface increased with the polarity of the solvent. This behaviour reflects the tendency of organic solvents to strip water molecules from the enzyme surface, reducing the enzyme activity [12,14]. Simulations performed with cutinase reveal the formation of water clusters on the protein surface [12]. The size of these clusters increases as the solvent polarity decreases. As expected, the water clusters hydrated the charged and polar residues located at the surface of the protein.

In this study, molecular dynamics simulations were performed to obtain a molecular description of the structural and dynamical changes exerted by a non-aqueous solvent (MeCN) in subtilisin Carlsberg (sCa). The simulations were designed to take into account the effect of MeCN in the protein with and without the inclusion of essential water. As defined by the simulation scheme described below, the inclusion of essential water corresponds to a 4.6% w/w hydration of the enzyme. The results obtained provided a detailed description of the structural changes occurring in the protein due to solvent–protein interactions. In order to have an idea of possible changes in the enzyme activity, the effect caused by the solvent in the structure of the oxyanion hole was monitored.

## 2. Methods

We have investigated the structure and dynamics of the serine protease sCa in several environments. Table 1 summarises the details of the modelled environments, where the amount of water molecules in each of the systems was varied. Specifically, the first and third systems studied had the protein in an aqueous media and in an organic solvent, respectively, whereas the second system conserved the essential water in the organic solvent as described below. Although the third system might not be prepared experimentally because even after lyophilisation treatment the system will conserve some water molecules, it was considered here as an extreme case corresponding to exposure to organic solvent for very long periods of time. The starting structure and coordinates of sCa were downloaded from the Protein Data Bank (PDB code: 1SCN) [15,16]. All the simulations were performed using the GROMACS simulation package [17,18]. For the non-aqueous systems, a three-site model with the same moment of inertia as MeCN was used to provide the description of the solvent molecule [19]. The downloaded protein structure included 141 water molecules from which 65 were used to perform the simulation with MeCN. The selection of these 65 water molecules was based on the amount of water present in the structure of sCa in anhydrous dioxane (PDB code: 1AF4) [20]. These molecules, termed 'essential' water, are located primarily at the surface of the protein. This number of molecules has been found to be necessary for the protein to conserve its catalytic activity in a non-aqueous environment [21–23]. Also, five water molecules between 3.5 and 4.0 Å from the ions present in the crystal structure were preserved, for a total of 70 essential water molecules. The SPC water model [24] was used to simulate the water present in the MeCN simulations and for the solvent in the aqueous system. Periodic boundary conditions were used in all directions.

Since we expected to observe a high degree of unfolding in the protein, the system was placed in a cubic box with a distance of 5.0 nm from its periodic image, preventing any interaction between them. The energy of the systems was minimised with the steepest descent algorithm, and 600 ps of position restrain dynamics was performed. The final system configuration generated from this procedure was used as a starting point for the production run. The GROMOS96 43a1 force field [25,26]

Table 1. The simulated systems: (i) the enzyme with ions in water (sCa—$H_2O$), (ii) enzyme with ions and surface waters in MeCN (sCa—MeCN) and (iii) enzyme with ions in MeCN (sCa—$MeCN_{NW}$).

| | | Ions | | | | |
|---|---|---|---|---|---|---|
| System name | Water molecules | $Ca^{2+}$ | $Na^+$ | $Cl^-$ | Solvent | Solvent molecules |
| sCa—$H_2O$ | 141 | 2 | 1 | *4* | $H_2O$ | 36,093 |
| sCa—MeCN | 70 | 2 | 1 | *4* | MeCN | 10,638 |
| sCa—$MeCN_{NW}$ | 0 | 2 | 1 | *4* | MeCN | 10,661 |

The italicised numbers correspond to the ions added to neutralise the total system charge.

was used for all systems, and all simulations were carried out at constant temperature, pressure and number of molecules. To maintain the temperature at 298 K and pressure at 1 atm, Berendsen weak coupling was used, with a coupling constant of 0.1 ps for temperature and 0.5 ps for the pressure [27]. A twin-range cut-off of 0.9/1.4 nm for van der Waals interactions was applied, and the particle mesh Ewald algorithm was used for long-range electrostatic interactions [28]. Neighbour lists were utilised and updated every five steps, and all protein and water bond lengths were constrained using the LINCS and SETTLE algorithm, respectively [29,30]. A time step of 2 fs was used in all simulations, with a total simulation time of 30 ns for the system with water as a solvent, and 92 ns for the systems with MeCN. The coordinates were saved every picosecond, and were analysed using the GROMACS v. 3.2.1 simulation package [17,18]. The molecular graphics images were generated using the Visual Molecular Dynamics software [31]. To characterise quantitatively the global flexibility of the protein, the Lindemann's disorder index, $\Delta_L$, was computed considering all the atoms present in the enzyme. This value was obtained using the following equation:

$$\Delta_L = \frac{1}{a'}\left(\frac{\sum_i \langle \Delta r_i^2 \rangle}{N}\right)^{1/2}, \quad (1)$$

where $a'$ is the most probable non-bonded near-neighbour distance, $N$ is the number of atoms and $\Delta r_i$ stands for the fluctuation in position of atom $i$ from its average position. Lindemann's disorder index has been shown to be useful in determining the flexibility and stability of proteins [32,33]. Specifically, if the value of $\Delta_L$ is between 0.1 and 0.14, the protein has a solid-like nature (low flexibility), whereas for values higher than 0.14, the protein behaves in a liquid-like form (high flexibility) [32–34].

To obtain information related to how much the structure of the protein deviates from the crystal, the root-mean-square deviation analysis (RMSD) and the root-mean-square fluctuations (RMSF) were computed. The RMSD was computed as a function of time, and as in previous studies it was used to monitor the convergence of the simulation. It has been extensively discussed in the literature that when the RMSD oscillates around a constant value (variation of 3 Å) the system has converge to a stable of metastable state, and hence the simulation can be terminated. In this study, this criterion was used to determine the extension of the simulations performed. The RMSD computed was determined as a function of residues and it provided information of structural variations in specific regions of the protein. The time evolution of the radius of gyration ($R_{gyr}$) and solvent accessible surface area (SASA) were monitored during the simulation. The averages for these properties were computed for the last 6 ns of the simulation. As explained in previous studies [35], if the simulation reaches RMSD that oscillates around a constant value (variation smaller than 3 Å), it can be assumed that the system has converged to a stable or a metastable state. Thus, during the discussion, we are going to use equilibrium or stable state as a way to describe that the system has converged to one of these configurations.

The SURFNET package [36] was used to calculate volumes of certain regions of the protein. The program defines the path volume by filling the empty regions with spheres of a variable radius. We chose a minimum radius for the gap spheres of 0.8 Å and a maximum of 4.0 Å. The spheres were then used to calculate a three-dimensional density map, using a grid separation of 0.8 Å.

## 3. Results and discussion

As stated, the RMSD values were used to obtain information related to how much the structure of the protein deviates from the X-ray crystalline structure in the different environments. Figure 1 shows the variation in RMSD as a function of time for the sCa—$H_2O$ (panel (a)) and the organic solvent (panel (b)) systems, where the sCa—MeCN and sCa—$MeCN_{NW}$ are coloured grey and black, respectively. The sCa—$H_2O$ system reached a constant RMSD value at approximately 30 ns, whereas the protein in the organic solvent was run for 92 ns to reach a stable or metastable state. The average values computed over the last 6 ns of the simulation for sCa—$H_2O$, sCa—MeCN and sCa—$MeCN_{NW}$ were 0.20, 0.55 and 0.50 nm, respectively. It was observed that the values of RMSD for sCa—MeCN and sCa—$MeCN_{NW}$ increased by 64 and 59%, respectively, when compared with the one obtained for sCa—$H_2O$. These results reveal a considerable change in the structure of the protein when it interacts with the organic solvent. On the other hand, the variation in the structure of the protein in the two MeCN systems showed different trends during the course of the simulation. Specifically, during the first 30 ns the sCa—$MeCN_{NW}$ system displayed larger structural changes than the sCa—MeCN, agreeing with previous simulation studies performed with subtilisin in MeCN that suggested that the absence of essential water slightly increases the RMSD value of the protein [3]. However, from 30 to 92 ns of simulation time the changes in the structure of the protein for the sCa—MeCN system were larger than for sCa—$MeCN_{NW}$, with an 11% increment during the last 6 ns. Hence, the essential water, or low water content, slightly increased the changes in the structure of the protein within this timescale. These results are in agreement with the results obtained by Micaelo and Soares [12], where cutinase was studied under various organic solvent at different hydration content. They observed small changes in the structure of the protein from that of the crystal when low water contents (>10% w/w) were used in MeCN.

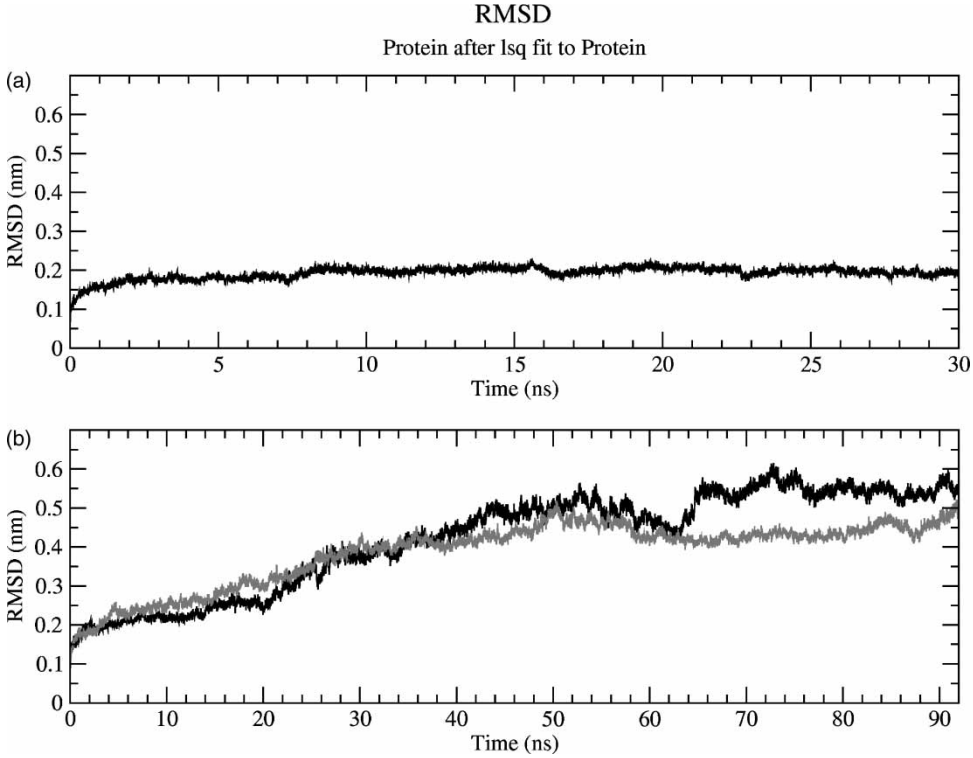


Figure 1. RMSD time evolution of sCa—$H_2O$ (panel (a)), sCa—MeCN (panel (b), grey) and sCa—$MeCN_{NW}$ (panel (b), black).

In order to obtain information related to the variation in the flexibility of the protein in the various environments, the Lindemman disorder index was computed. Our results showed that sCa—$H_2O$ was the least flexible system with a value of $\Delta_L = 0.12$, whereas sCa—MeCN and sCa—$MeCN_{NW}$ showed higher flexibility with values of $\Delta_L$ of 0.17 and 0.19, respectively – an increment of 31 and 37%, respectively, when compared with the aqueous system. Hence, changing the solvent from water to MeCN caused a significant increment in the flexibility of the protein, which is in accordance with the significant change in the structure observed in the organic solvent.

Figure 2 shows the RMSF as a function of amino acids average over the last 6 ns. From the different panels, it can be observed that both MeCN systems exhibited considerable changes in most amino acids compared with the sCa—$H_2O$ system, with a significant increment in the values of RMSF for the surface loops. When the two systems with MeCN as a solvent are compared (Figure 2(d)), it can be observed that the sCa—MeCN system exhibited higher values of RMSF in the residues comprising the 100–120 and 130–140 amino acid sequence, while the sCa—$MeCN_{NW}$ showed higher deviations in the 150–170, 185–200 and 300–330 regions. The sCa—$MeCN_{NW}$ system exhibited considerable changes primarily in two regions near the surface loops, which involve residues 103–108 and 130–140. The first region overlapped the α-helix 4 (H4), which includes residues 103–107, while the latter include residues forming the α-helix 5 (H5), which is composed of residues 132–146. The variations in these regions in the sCa—MeCN system were negligible. Detailed analysis of the structural modifications previously described on this system shows that the H5 helix undergoes a partial unfolding of residues 132–134, caused mainly by the translation of the loop formed by residues 124–131. This translation induced a change in the orientation of the carbonyl oxygen of residue Ser-131, breaking the helical hydrogen bond with the amide hydrogen of residue Thr-132. This change is the first step of a chain effect leading to the transformation from α-helix to random coil of the region. The amino acid residues comprising the H4 followed the same unfolding behaviour caused by the increment in flexibility towards the end of the loop in residues 92–104. Clearly, these results indicate that MeCN is interacting with the protein, and hence inducing changes in different regions of the protein. The changes occurring depend on the presence of essential water and consequently the surface residues have different chain rearrangements for both systems.

The conformational changes previously described were confirmed by the values obtained for SASA and $R_{gyr}$, which are closely related to each other because as the size of the system decreases, the surface area-to-volume ratio decreases. Specifically, the values of $R_{gyr}$ for

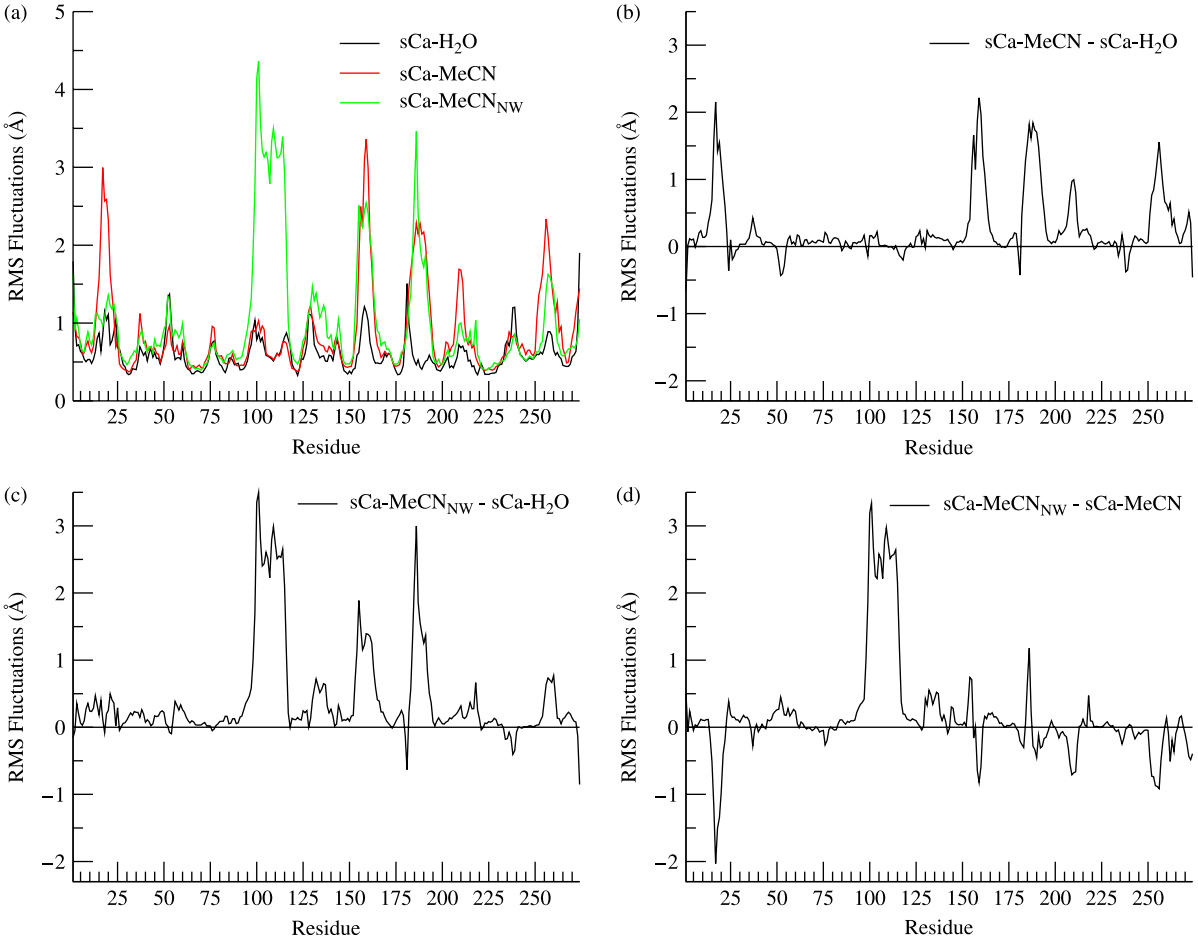


Figure 2. RMSF by residue about the $C_\alpha$ time average structure for the last 6 ns of the simulation: (panel (a)) all the systems, (panel (b)) differences between sCa—MeCN and sCa—$H_2O$ systems, (panel (c)) differences between sCa—$MeCN_{NW}$ and sCa—$H_2O$ and (panel (d)) difference between sCa—$MeCN_{NW}$ and sCa—MeCN systems.



sCa—$H_2O$, sCa—MeCN and sCa—$MeCN_{NW}$ are 1.63, 1.79 and 1.78 nm, respectively, and the SASA values are 105, 154 and 153 $nm^2$, respectively. Clearly, for the MeCN systems, an increment in these structural properties was observed, suggesting a change in the tertiary structure of the protein. This increment in size can be attributed to the discussed motion of the surface loops, which gives a more open conformation.

Interestingly, a detailed analysis of snapshot configurations showed that the structural changes occurring in the various systems opened a path for the solvent to the protein's core. The opening of this path is shown in Figure 3, where the conformations adopted by various loops are shown by a surface representation, i.e. loops L1 and L2 for the sCa—$H_2O$ (panel (a)), sCa—MeCN (panel (b)) and sCa—$MeCN_{NW}$ (panel (c)). Evidently, the L1 and L2 loops moved away from each other in the MeCN systems, adopting a conformation that opened a path to the protein core. This opening is the result of residues Gly(100), Ser(101), Tyr(104) and Ser(130) changing its orientation, as well as a peptide bond displacement. As the number of water molecules decreases in the system, the aperture becomes larger. Moreover, the aperture between the loops in the sCa—MeCN system was detected only after a certain number of water molecules were removed from the protein surface by MeCN. The movement of the L1 loop also affected the Xe-binding site previously identified by Prage et al. [37], primarily due to changes in orientation and conformation of the Leu-126, which is common to both the opened path and the Xe pocket. Moreover, some of the residues comprising this pocket also coincide with residues in the oxyanion hole near the catalytic triad.

In Figure 3, the distance between the loops and the path volume representation (grey) showed that the aperture is larger in the sCa—$MeCN_{NW}$ than in the other two systems, making the protein core more accessible to the organic solvent. The path volumes obtained for the openings were 434, 735 and 775 $Å^3$ for the sCa—$H_2O$, sCa—MeCN and sCa—$MeCN_{NW}$, respectively. This result corroborates that large amounts of solvent could reach the protein core in the

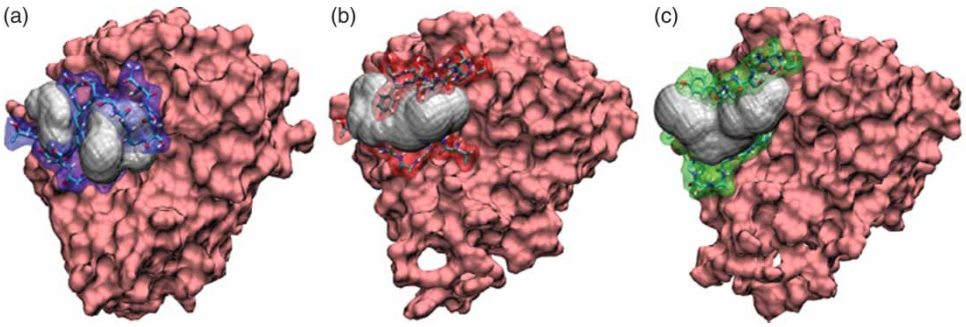


Figure 3. Surface representation of the sCa—$H_2O$ (a), sCa—MeCN (b) and sCa—$MeCN_{NW}$ (c) systems. The amino acid residues comprised in the L1 (96–104) and L2 (125–132) sequences are highlighted with blue, red and green for the sCa—$H_2O$, sCa—MeCN and sCa—$MeCN_{NW}$, respectively. The volume of the path (grey) is highlighted for a better appreciation of the generated path.

sCa—$MeCN_{NW}$ system, thus inducing significant conformational changes in the protein, ultimately affecting the enzyme activity. The above result is relevant to molecular description in enzymology because solvation of the protein core has been identified as an important step in the unfolding process [38], which decreases the enzyme activity and stability.

It is important to mention that it was expected that both MeCN systems converge to the same average configuration, i.e. if the essential water was being stripped from sCa—$MeCN_{NW}$, then the system should be similar to sCa—MeCN. However, our results showed that these systems have slightly different structural and dynamical properties. The reason for this is that the conformational changes occurred by two different mechanisms and in the timescale of our simulation, two different metastable states were reached.

Figure 4 shows the time evolution of the number of water (panel (a)) and MeCN (panel (b)) molecules for the sCa—MeCN system within 2.7 Å of the protein surface. It can be observed in Figure 4(a) that during the simulation, the amount of water on the enzyme's surface decreased due to the high dielectric constant of the organic solvent. The organic solvent strips away water molecules from the protein surface to the bulk solvent during the first 50 ns. Hence, initially the organic solvents primarily interact with

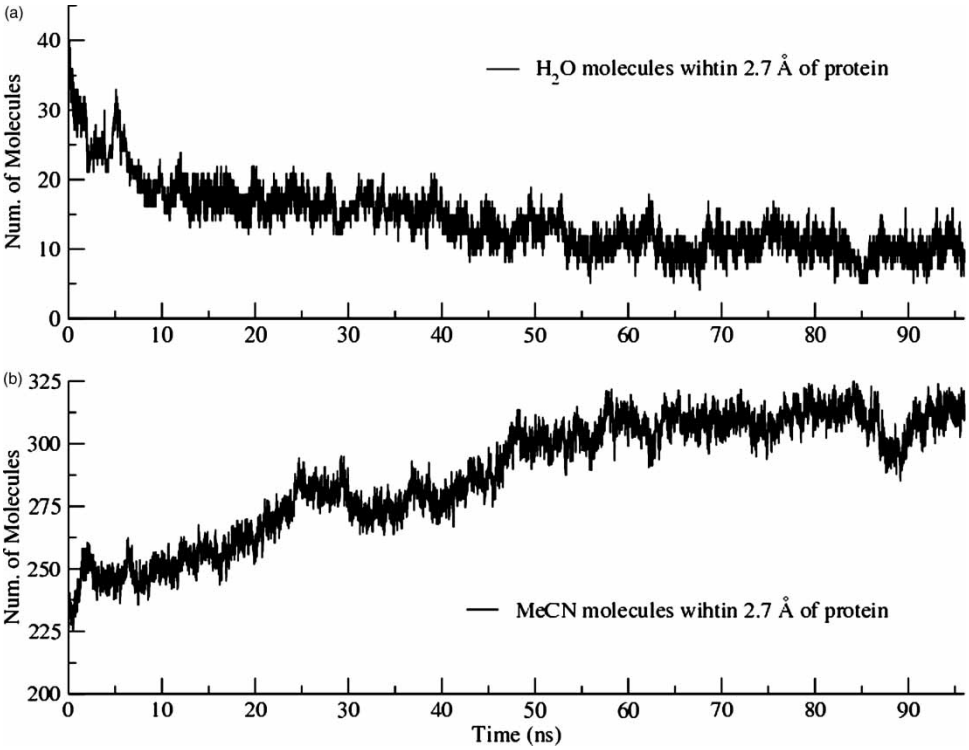


Figure 4. Number of water (a) and solvent (b) molecules within 2.7 Å of the protein surface for the sCa–MeCN system.

Table 2. Calculated average distance between atoms of catalytically important residues in the active site.

| Distance global average | | | |
|---|---|---|---|
| | Distance (Å) | | |
| Atom pairs | sCa—$H_2O$ | sCa—MeCN | sCa—$MeCN_{NW}$ |
| Asn-155*ND*:Ser-221*ND* | 4.4 (0.5) | 8.0 (1) | 11.0 (1) |
| His-64*HD1*:Asp-32*OD1* | 2.2 (0.2) | 2.1 (0.2) | 2.2 (0.2) |
| His-64*HD*1:Asp-32*OD2* | 2.3 (0.2) | 2.3 (0.2) | 2.0 (0.2) |
| Ser-221*HG*:His-64*NE2* | 3.5 (0.6) | 1.9 (0.2) | 1.9 (0.4) |

the enzyme water layer on the surface rather than with the enzyme itself [8]. Beyond this point, the structure of subtilisin started to undergo structural changes due to the entrance of MeCN into its core. As observed in Figure 4(b), a continuous increase of solvent molecules inside the protein was observed until 50 ns, when an average of 311 MeCN molecules was reached. Consequently, the lack of water facilitates the organic solvent entrance to the protein, thus causing a direct disruption of the structure of this system.

An important factor to be considered in an enzymatic system is the variation of the active site due to the interaction with the solvent. Our results showed that the structural changes suffered in the different systems do not affect all the residues present in the active site of the enzyme. Table 2 shows the average distance between atoms of catalytically important residues (catalytic triad). The conformation between the atoms involved in the catalytic triad in all systems maintained a favourable distance to form the hydrogen bond (2–3.5 Å) necessary to carry out its function. The major disruption observed in the active site of the systems containing MeCN as solvent was a change in the orientation of the Asn-155. Usually, to be catalytically effective this residue chain points to the catalytic triad. However, in the MeCN systems the chain rotates, pointing to the loop comprising residues 156–163, which cause a disruption of the oxyanion hole and the Xe pocket. The disruption of the oxyanion hole will affect the enzyme's activity as various experimental [8,39] and theoretical [40] studies have identified. The reason for this is that the rate-limiting step in the enzymatic activity of this protein is related to the stabilisation of a tetrahedral intermediate, which involves the oxyanion hole. Since the side chain of the Asn-155 will not participate in the stabilisation of the tetrahedral intermediate, it has been postulated that the reaction rate is affected.



## Acknowledgements

The authors acknowledge the High Performance Computing Facility of the University of Puerto Rico. G.L.B. acknowledges support of the NIH/SCORE (Grant No. S06 GM08102) and NIH/INBRE (Grant No. P20 RR-016470) programmes. G.E.L. acknowledges support of the NIH/SCORE (Grant No. 5S06GM08103-35) programme and NIH/INBRE (Grant No. P20 RR-016470).

## Notes

1. Email: ancruz@uprm.edu
2. Email: asantana@uprm.edu
3. Email: gl_barletta@webmail.uprh.edu
4. Email: glopez@uprm.edu

## References

[1] K. Griebenow, Y. Díaz, A.M. Santos, I. Montanez, L. Rodríguez, M.W. Vidal, and G. Barletta, *Improved enzyme activity and enantioselectivity in organic solvents by methyl-cyclodextrin*, J. Am. Chem. Soc. 121 (1999), pp. 8157–8163.

[2] Y.L. Khmelnitsky and R.O. Rich, *Biocatalysis in nonaqueous solvent*, Curr. Opin. Chem. Biol. 3 (1999), pp. 47–53.

[3] Y.J. Zheng and R.L. Ornstein, *Molecular dynamics of subtilisin Carlsberg in aqueous and nonaqueous solutions*, Biopolymers 38 (1996), pp. 791–799.

[4] P. Sears, K. Witte, and C.H. Wong, *The effect of counter ion, water concentration, and stirring on the stability of subtilisin BPN' in organic solvent*, J. Mol. Catal. B Enzym. 6 (1999), pp. 297–304.

[5] G. Colombo and G. Carrea, *Modeling enzyme reactivity in organic solvents and water through computer simulations*, J. Biotechnol. 96 (2002), pp. 23–33.

[6] J.L. Scmitke, C.R. Wescotty, and A.M. Klibanov, *The mechanistic dissection of the plunge in enzymatic activity upon transition from water to anhydrous solvent*, J. Am. Chem. Soc. 118 (1996), pp. 3360–3365.

[7] I. Montañez, E. Alvira, M. Macias, A. Ferrer, M. Fonceca, J. Rodríguez, A. González, and G. Barletta, *Enzyme activation in organic solvents: Co-Lyophilization of subtilisin Carlsberg with methyl-cyclodextrin renders an enzyme catalyst more active that the cross-linked enzyme crystal*, Biotechnol. Bioeng. 78(1) (2002), pp. 53–59.

[8] J.K. Amisha, T. Xia, S. Kumar, L. Zhao, and A.H. Zewail, *Enzyme functionality and solvation of subtilisin Carlsberg: from hours to femtoseconds*, Chem. Phys. Lett. 387 (2004), pp. 209–215.

[9] C.M. Claudio, V.H. Texeira, and A.M. Baptista, *Protein structure and dynamics in nonaqueous solvents: Insights from molecular dynamics simulations studies*, Biophys. J. 94 (2003), pp. 1628–1641.

[10] N.M. Micaelo, V.H. Texeira, A.M. Baptista, and C.M. Soares, *Water dependent properties of cutinase in nonaqueous solvents: a computational study of enantioselectivity*, Biophys. J. 89 (2005), pp. 999–1008.

[11] N.M. Micaelo and C.M. Soares, *Protein structures and dynamics in ionic liquid, insights from molecular dynamics simulation studies*, J. Phys. Chem. B 112 (2008), pp. 2566–2572.

[12] N.M. Micaelo and C.L. Soares, *Modeling hydration mechanisms of enzyme nonpolar and polar organic solvents*, FEBS J. 274 (2007), pp. 2424–2436.

[13] P.P. Wangikar, P.C. Michels, D.S. Clark, and J.S. Dordick, *Structure and function of subtilisin BPN' solubilized in organic solvents*, J. Am. Chem. Soc. 119 (1997), pp. 70–76.
[14] L. Yang, J.S. Dordick, and S. Garde, *Hydration of enzyme in nonaqueous media is consistent with solvent dependence of its activity*, Biophys. J. 87 (2004), pp. 812–821.
[15] H.M. Berman, J. Westbrook, Z. Feng, G. Gilliland, T.N. Bhat, H. Weissig, I.N. Shindyalov, and P.E. Bourne, *The protein data bank*, Nucleic Acids Res. 28 (2000), pp. 235–242.
[16] A.C. Steinmetz, H.U. Demuth, and D. Ringe, *Inactivation of subtilisin Carlsberg by* N-*((tert-butoxycarbonyl)alanylprolylphenylalanyl)-Obenzoylhydroxyl-amine: formation of a covalent enzyme–inhibitor linkage in the form of a carbamate derivative*, Biochemistry 33 (1994), pp. 10535–10544.
[17] H.J.C. Berendsen, D. van der Spoel, and R. van Drunen, *GROMACS: A message passing parallel molecular dynamics implementation*, Comput. Phys. Commun. 91 (1995), pp. 43–56.
[18] E. Lindahl, B. Hess, and D. van der Spoel, *Gromacs 3.0: a package for molecular simulation and trajectory analysis*, J. Mol. Model. 7 (2001), pp. 306–317.
[19] E. Guardia, R. Pinzón, J. Casulleras, M. Orozco, and F.J. Luque, *Comparison of different three site interaction potentials for liquid acetonitrile*, Mol. Simul. 26 (2001), pp. 287–306.
[20] J.L. Schmitke, L.J. Stern, and A.M. Klibanov, *The crystal structure of subtilisin Carlsberg in anhydrous dioxane and its comparison with those in water and acetonitrile*, Proc. Natl Acad. Sci. USA 94 (1997), pp. 4250–4255.
[21] A. Zacks and A.M. Klibanov, *Enzymatic catalysis in nonaqueous solvents*, J. Biol. Chem. 263 (1988), pp. 3194–3201.
[22] M.A. Klibanov, *Enzymatic catalysis in anhydrous organic solvents*, Trends Biochem. Sci. 14 (1989), pp. 141–144.
[23] G. Colombo, S. Toba, and K.M. Merz, Jr, *Rationalization of enantioselectivity of subtilisin in DMF*, J. Am. Chem. Soc. 121 (1999), pp. 3486–3493.
[24] J. Hermans, H.J.C. Berendsen, W.F. van Gunsteren, and J.P.M. Postman, *A consistent empirical potential for water–protein interactions*, Biopolymers 23(8) (1984), pp. 1513–1518.
[25] W.R.P. Scott, P.H. Hunenberger, I.G. Tironi, A.E. Mark, S.R. Billeter, J. Fennen, A.E. Torda, T. Huber, P. Kruger, and W.F. van Gunsteren, *The GROMOS biomolecular simulation program package*, J. Phys. Chem. A 103 (1999), pp. 3596–3607.
[26] W.F. van Gunsteren and H.J.C. Berendsen, *Computer simulation of molecular dynamics: methodology, applications, and perspectives in chemistry*, Angew Chem., Int. Ed. 29 (1990), pp. 992–1023.
[27] H.J.C. Berendsen, J.P.M. Postman, W.F. van Gunsteren, A. DiNola, and J.R. Haak, *Molecular dynamics with coupling to an external bath*, J. Chem. Phys. 81 (1984), pp. 3684–3690.
[28] U. Essmann, L. Perera, M.L. Berkowitz, T. Darden, H. Lee, and L.G. Pedersen, *A smooth particle mesh Ewald potential*, J. Chem. Phys. 103 (1995), pp. 8577–8592.
[29] B. Hess, H. Bekker, H.J.C. Berendsen, and J.G.E.M. Fraaije, *LINCS: a linear constraint solver for molecular simulations*, J. Comp. Chem. 18 (1997), pp. 1463–1472.
[30] S. Miyamoto and P.A. Kollman, *SETTLE: an analytical version of the SHAKE and RATTLE algorithms for rigid water models*, J. Comput. Chem. 13 (1992), pp. 952–962.
[31] W. Humphrey, A. Dalke, and K. Schulten, *VMD – Visual molecular dynamics*, J. Mol. Graph. 14 (1996), pp. 33–38.
[32] Y. Zhou and M. Karplus, *Folding thermodynamics of a model three-helix bundle protein*, Proc. Natl Acad. Sci. USA 94 (1997), pp. 14429–14432.
[33] M. Rueda, C. Ferrer-Costas, T. Meyer, A. Perez, J. Campus, A. Hospital, L.J. Gelpi, and M. Orozco, *A consensus view of protein dynamics*, Proc. Natl Acad. Sci. USA 104 (2007), pp. 796–801.
[34] F.H. Stillinger, *A topographic view of supercooled liquids and glass formation*, Science 267 (1995), pp. 1935–1939.
[35] E. Villa, A. Balaef, and K. Schulten, *Structural dynamics of the lac repressor–DNA complex revealed by a multi scale simulation*, Proc. Natl Acad. Sci. USA 102 (2005), pp. 6783–6788.
[36] R.A. Laskowski, *Surfnet – A program for visualizing molecular surfaces, cavities, and intermolecular interactions*, J. Mol. Graph. 13 (1995), pp. 323–330.
[37] T. Prangé, M. Schultz, L. Pernot, N. Colloc'h, S. Longhi, W. Bouriet, and R. Fourme, *Exploring hydrophobic sites in proteins with xenon or krypton*, Proteins 30 (1998), pp. 61–73.
[38] G. Colombo and K.M. Merz, Jr., *Stability and activity of mesophilic subtilisin E and its thermophilic homolog: Insights from molecular dynamics simulation*, J. Am. Chem. Soc. 121 (1999), pp. 6895–6903.
[39] K.M. Bobofchak, A.O. Pineda, F.S. Mathews, and E.D. Cera, *Energetic and structural consequences of perturbing Gly-193 in the oxyanion hole of serine proteases*, J. Biol. Chem. 280(27) (2005), pp. 25644–25650.
[40] T. Ishida and S. Kato, *Theoretical perspectives on the reaction mechanism of serine proteases: The reaction free energy profiles of the acylation process*, J. Am. Chem. Soc. 125 (2003), pp. 12035–12048.